J Incl Phenom Macrocycl Chem (2007) 57:519–523
DOI 10.1007/s10847-006-9243-6

ORIGINAL ARTICLE

The modes of complexation of benzimidazole with aqueous β-cyclodextrin explored by phase solubility, potentiometric titration, ^{1}H-NMR and molecular modeling studies

F. O. Yousef · M. B. Zughul · A. A. Badwan

Received: 15 May 2006 / Accepted: 20 October 2006 / Published online: 18 January 2007

Abstract The results of rigorous modeling of phase solubility diagrams, pH solubility profiles and potentiometric titrations revealed the following for benzimidazole (**BZ**) and **BZ**/β-CD complexation in aqueous solution: (a) the pK_a value of **BZ** estimated at 5.66 ± 0.08 was reduced to 5.33 ± 0.06 in the presence of 15 mM β-CD at 25 °C, thus indicating inclusion complex formation; (b) **BZ** forms soluble 1:1 and 2:1 **BZ**/β-CD complexes with complex formation constants K_{11} = 104 ± 8 M^{-1} and K_{21} = 16 ± 6 M^{-1}; (c) protonated BZ forms only 1:1 complex with K_{11} = 42 ± 12 M^{-1}; (d) ^{1}H-NMR studies in D_2O showed significant upfield chemical shift displacements for inner cavity β-CD protons indicating inclusion complex formation, while (e) Molecular modeling of **BZ**-β-CD interactions in water clearly indicated complete inclusion of one **BZ** molecule into the β-CD cavity.

Keywords Benzimidazole · β-cyclodextrin complexes · Complex formation constants · ^{1}H-NMR · molecular modeling · Phase solubility · pH-solubility profile · Potentiometric titration

F. O. Yousef
Hayat Pharmaceutical Industries, Amman, Jordan

M. B. Zughul (✉)
Department of Chemistry, University of Jordan, Amman, Jordan
e-mail: mbzughul@ju.edu.jo

A. A. Badwan
The Jordanian Pharmaceutical Manufacturing Company, Naor, Jordan

Introduction

Benzimidazole (**BZ**) serves as a common moiety for a large number of biologically active compounds including antihistaminic, anti-emetic, anthelmintic and antifungus drugs, in addition to vitamin B_{12} [1]. Our interest in exploring possible mechanisms of solubility enhancement exerted by aqueous β-cyclodextrin (β-CD) on some water-insoluble **BZ**-derivatives led to investigate the contribution of **BZ** to their complexation modes. The measured phase solubility diagram of **BZ** against β-CD concentration in water appeared quite linear with a slope exceeding unity (1.17) indicating formation of S_nL-type soluble complex formation (S = **BZ**, L = β-CD, $n > 1$). This work reports the results of an investigation of **BZ**/β-CD complexation in aqueous solution by phase solubility studies, pH solubility profiles, potentiometric titrations, ^{1}H-NMR spectrometry and molecular modeling of **BZ**-β-CD interactions.

Materials and methods

Materials

Benzimidazole (**BZ**) was of AR grade from Riedel-De Haën, β-cyclodextrin (pharmaceutical grade) from AVEBE. All other chemicals were of analytical grade. Doubly distilled deionised water was used throughout.

Methods

Instrumentation

UV/Visible spectrophotometer (Beckman DU-70/USA), Thermostatic shaker (Julabo SW-21C/Germany),

300 MHz FT-NMR spectrometer (Bruker, Avance DPX300/Germany), Automatic titrator (Mettler DL 67/ Switzerland), and pH-meter (SCHOTT CG840/ Germany).

pH-solubility profiles

Equal amounts of **BZ** in excess of its inherent solubility were added to 50 mL of 1.0 M phosphate buffer solutions at different pHs and 25 °C. The solutions were thermostatically shaken, let to settle, filtered and the UV/Visible absorbance measured. The concentration of each solution was determined using appropriate calibration curves.

Phase solubility studies

Phase solubility studies were carried out according to Higuchi and Connors [2]. Phase solubility diagrams were obtained where excess amounts of **BZ** were added to flasks containing 50.0 mL 0.1 M phosphate buffer, 0.1 M NaCl, solutions at 25 °C having different β-CD concentrations. The solutions were thermostatically shaken, let to settle, filtered and the absorbance measured. The concentration of each solution was determined spectrophotometrically against appropriate calibration curves. Analysis of phase solubility diagrams to estimate complex formation constants were conducted using rigorous regression procedures reported earlier [3, 4].

Potentiometric titrations

A sample weighing 0.1181 g of **BZ** dissolved in 50 mL water (0.02 M) was titrated at 25 °C with aqueous 0.2 M HCl, where the pH was monitored against the volume of titrant added at a 0.005 mL resolution and 0.1 mV accuracy for the equivalence point detection. Another 50 mL of aqueous 15 mM β-CD solution saturated with **BZ** (54.4 mM) was similarly titrated. Nonlinear regression of the experimental data yielded the pK_a values of **BZ** and the corresponding pK_a value of the **BZ**/β-CD complex.

^{1}H-NMR

Appropriately weighed samples **BZ**, β-CD, and the corresponding freeze-dried **BZ/**β-CD complex were dissolved in D_2O, and the 300 MHz ^{1}H-NMR spectra were obtained at 25 °C. The chemical shift displacements ($\Delta\delta$ in ppm) of β-CD protons on complexation ($\Delta\delta = \delta_{complex} - \delta_{\beta\text{-CD}}$) were thus determined.

Molecular mechanical modeling

Molecular modeling simulations of **BZ**/β-CD interactions in a water box of periodic boundary conditions were conducted using the Hyperchem® molecular modeling software (release 6.03 professional, Hypercube Inc., Waterloo, Canada). Both Amber and enhanced MM Force fields implementing the atomic charges or bond dipoles options for calculation of electrostatic interactions were used in these computations. Partial atomic charges were obtained by means of AM1 semi-empirical calculations [5]. Energy minimization was performed using the conjugate gradient algorithm (0.01 kcal/mol Å gradient). The initial molecular geometry of β-CD was obtained using X-ray diffraction data [6–9], which was then energetically optimized using the Amber force field by imposing a restraint on the dihedral angles to the average values [6]. The **BZ** molecule was built up from standard bond lengths and bond angles, which was further optimized with the Amber and MM force fields.

The previously optimized structures of **BZ** and β-CD molecules in the water box were allowed to approach each other along the symmetric x-axis passing through the center of the β-CD cavity. The imidazole side of **BZ** was allowed to approach through both wide and narrow rims of β-CD cavity. The energy of **BZ** was computed (while β-CD was fixed) at 1 Å intervals, starting at $x = -20$ Å all through $x = +20$ Å from the origin of the Cartesian coordinate, which was designated by the center of the ether glucoside oxygen atoms of β-CD and an atom closest to the center of mass of the **BZ** molecule. The binding energy ($E_{binding} = E_{complex} - \sum E_{components}$) was plotted against x for each longitudinal approach to indicate the energy minima. The whole **BZ**/β-CD system of minimum energy thus obtained was allowed to interact free of restrictions to either molecule to obtain the optimized 1:1 complex configuration whose energy was computed together with the van der Waals and electrostatic contributions.

To obtain the optimized 2:1 **BZ**/β-CD complex configuration, the already optimized **BZ** molecule was allowed to approach the 1:1 complex from the either side of β-CD molecule. The binding energy corresponding to the optimized configuration was similarly arrived at free of restrictions as discussed above.

Results and discussion

pH solubility profile and Phase solubility Diagrams

Figure 1 shows the pH-solubility profiles of **BZ** in the absence and presence of 15 mM β-CD obtained in

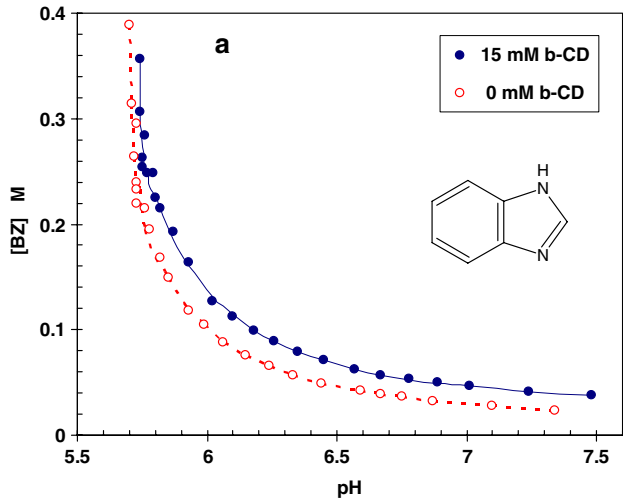

Fig. 1 pH-solubility profiles of **BZ** in the absence and presence of 15 mM β-CD obtained in 0.1 M phosphate buffer at 25 °C

phosphate buffer, while Fig. 2 depicts the PSD against β-CD concentration in water where pH varied from 7.50 to 7.84 at 25 °C. In nonlinear regression of the experimental data, the following acid-base and complex equilibria were found relevant (*B* denotes free **BZ**, *L* denotes free β-CD, and *y* is the molar activity coefficient given by the Davies equation ($\log y = -0.51\, z^2([\sqrt{I}/(1+\sqrt{I})] - 0.3I$):

$$BH^+ \rightleftharpoons B + H^+; \qquad K_a = [B](H^+)/y[BH^+]$$

$$B + L \rightleftharpoons BL; \qquad K_{11} = [BL]/[B][L]$$

$$BL + B \rightleftharpoons B_2L; \qquad K_{21} = [B_2L]/[B][BL]$$

$$BH + L \rightleftharpoons BHL^+; \quad K'_{11} = [BHL^+]/[BH^+]$$

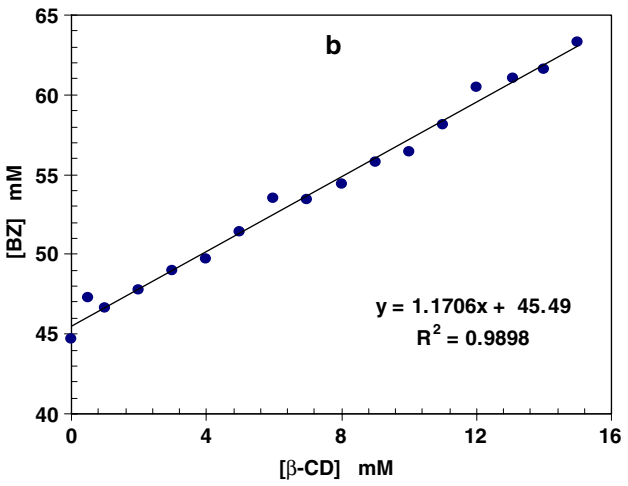

Fig. 2 Phase solubility diagram of **Bz**/β-CD in water (pH varies from 7.5 to 7.84) at 25 °C

The equilibrium concentrations of **BZ** and β-CD at a given pH are given according to:
(a) In the absence of β-CD:

$$[\mathbf{BZ}] = [B] + [BH^+] = [B](1 + (H^+)/yK_a) \qquad (1)$$

(b) In the presence of β-CD:

$$\begin{aligned}[\mathbf{BZ}] &= [B] + [BH^+] + [BL] + 2[B_2L] + [BH^+] \\ &= [B](1 + (H^+)/yK_a + K_{11}[L] \\ &\quad + 2K_{11}K_{21}[L] + K'_{11}\{(H^+)/yK_a\}[L] \qquad (2)\end{aligned}$$

$$\begin{aligned}[\beta - CD] &= [L] + [BL] + [B_2L] + [BHL^+] \\ &= [L]\left(1 + K_{11}[B] + 2K_{11}K_{21}[B] + K_{11\prime}(H^+)/yK_a\right)[L] \qquad (3)\end{aligned}$$

The free β-CD concentration, [L], is thus obtained from eq. 3 according to

$$\begin{aligned}[L] &= [\beta - CD]/(1 + K_{11}[B] + 2K_{11}K_{21}[B] \\ &\quad + K'_{11}(H^+) \,/\, y\, K_a)\end{aligned}$$

Since β-CD concentration is initially known, and the intrinsic solubility of neutral **BZ**, [B], is also known, both [L] and [B] are substituted back into Eq. 2 to obtain the predicted equilibrium **BZ** concentration $[\mathbf{BZ}]^{\text{Predicted}}$, and nonlinear regression of the experimental data is attained by minimizing the sum of squares of errors given by

$$Q = \sum_i \{[\boldsymbol{BZ})^{\text{Predicted}} - (\boldsymbol{BZ}]_{\text{measured}}\}^2.$$

For potentiometric titrations (Fig. 3), concentrations were adjusted for the volume of titrant added. Input values were crudely guessed from linear regression which for [B], pK_a, K_{11}, K_{21}, K'_{11}were 0.02, 5.5, 10, 10, 10, respectively. The results of nonlinear regression are listed in Table 1 for comparison purposes, which remarkably agree to within experimental error. Note that the lowering in pK_a value of **BZ** in aqueous β-CD solution provides evidence for inclusion complex formation.

^{1}H-NMR

^{1}H-NMR spectra indicate significant upfield chemical shift displacements ($\Delta\delta$) of β-CD protons in **BZ**/β-CD solution as shown in Table 2. Substantial upfield chemical shift displacements of the inner cavity protons (H_3 and H_5) in addition to proton H_6 of β-CD strongly indicate the formation of **BZ**/β-CD inclusion complexes in aqueous solution.

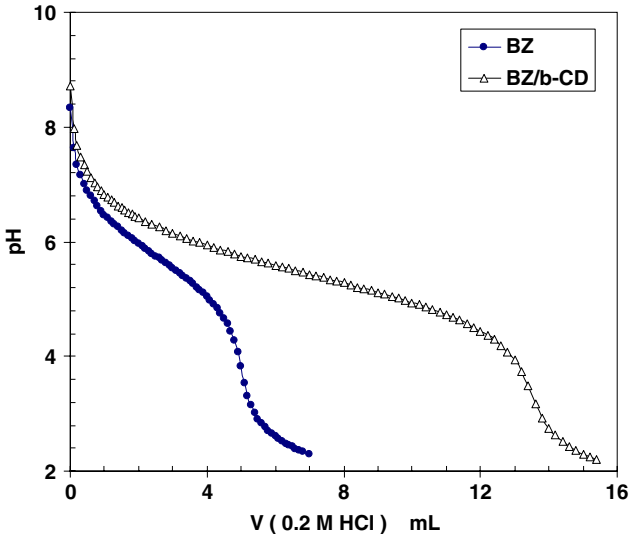

Fig. 3 Potentiometric acid-base titration with 0.20 M aqueous HCl of 50 mL aqueous 20 mM **BZ**, and of 50 mL of aqueous 15 mM β-CD saturated with **BZ** (54.4 mM) at 25 °C

Molecular mechanical modeling

Molecular modeling of **BZ**-β-CD interactions in a water box of periodic boundary conditions showed that the most stable conformational structure of the 1:1 **BZ**/β-CD complex involves complete inclusion of **BZ** into the β-CD cavity (Fig. 4). As to the optimized 2:1 complex, it shows that the second **BZ** molecule is peripherally associated with the 1:1 complex through hydrogen bond interaction of the **BZ** imidazole nitrogen with the secondary hydroxyl group network situated at the wide rim of the β-CD cavity (Fig. 4).

Conclusion

Nonlinear regression of pH solubility profiles, potentiometric titrations and phase solubility diagrams offer three techniques capable of ascertaining the formation and stoichiometry of soluble substrate/cyclodextrin inclusion complexes. The successful application of this methodology to systems exhibiting 2:1 complex stoichiometry was uniquely demonstrated through this study of the complexation of the highly soluble substrate (benzimidazole) with β-CD. Within the limits of experimental error, the three techniques converged to the same values of acid-base ionization constants and complex formation constants. The lowering in the pK_a value of benzimidazole in the presence of β-CD in solution indicates inclusion complexation. Moreover, ^{1}H-NMR chemical shift displacements of inner β-CD cavity protons of freeze-dried **BZ**/β-CD complex, combined with molecular modeling geometry optimizations of **BZ**-βCD inter-

Table 1 **BZ**/β-CD complex formation parameters obtained from (**a**) pH solubility profile of an aqueous 15 mM β-CD solution saturated with **BZ;** (**b**) potentiometric titrations; and (**c**) PSD of **BZ**/β-CD at 25 °C. (Numbers in brackets indicate confidence limits for a 95% confidence level)

parameter	pH-profile	Titration	PSD
pK_a	5.66 (0.08)	5.70 (0.06)	5.63 (0.08)
$pK_{a\ complex}$	5.3 (0.07)	5.3 (0.06)	5.3 (0.08)
K_{11} (M^{-1})	108 (6)	104 (8)	100 (8)
K_{21} (M^{-1})	15 (5)	16 (6)	18 (6)
K_{11}' (M^{-1})	44 (12)	40 (11)	43 (14)

Table 2 Changes in ^{1}H-NMR chemical shifts δ (ppm) of β-CD protons on complexation with **BZ** obtained in D_2O at 25 °C

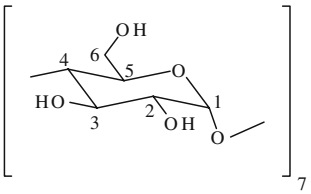

β-CD Proton	$\Delta\delta_{ppm}$
H_1	–0.055
H_2	–0.031
H_3	–0.104
H_4	–0.054
H_5	Overlapping
H_6	–0.133

Fig. 4 Side views of the optimized geometries of 1:1 and 2:1 **BZ**/β-CD complexes in water

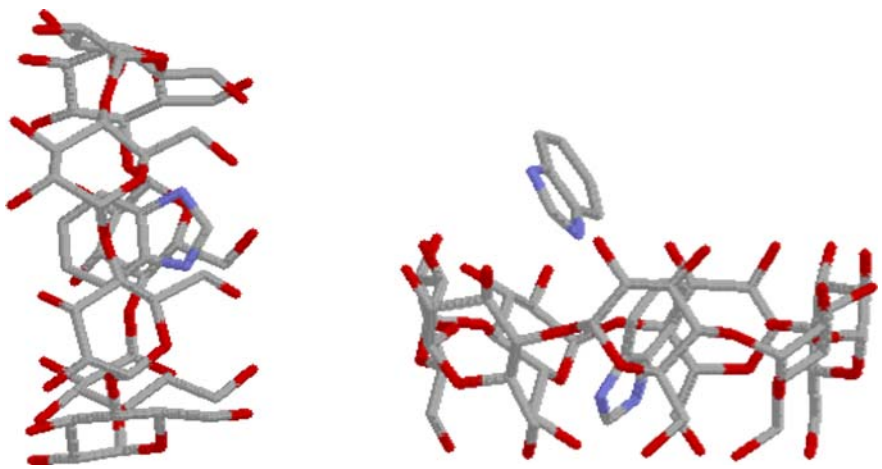

actions confirm the formation of soluble **BZ**/β-CD complexes in aqueous solution.

References

1. Preston, P.N., Smith, D.M., Tennant, G.: Benzimidazoles and Congeneric Tricyclic Compounds, Part I, John Wiley & sons, New York (1981), pp. 1–287
2. Higuchi, T., Connors, K.A.: Phase-solubility techniques. Advan. Anal. Chem. Instr. **4**, 117–212 (1965)
3. Zughul, M.B., Badwan, A.A.: Rigorous analysis of S_2L-type phase solubility diagrams to obtain individual formation and solubility product constants of both SL- and S_2L-type complexes. Int. J. Pharm., **151**, 109–119 (1997)
4. Zughul, M.B., Al-Omari, M., Badwan, A.A.: Thermodynamics of propylparaben/β-cyclodextrin inclusion complexes. Pharm. Develop. Tech. **3**, 43–53 (1998)
5. Dewar, M.J.S., Zoebisch, E.G., Healy, E.F., Stewart, J.J.P.: Development and use of quantum mechanical molecular models. 76. AM1: a new general purpose quantum mechanical molecular model. J. Am. Chem. Soc. **107**, 3902–3909 (1985)
6. Puliti, R., Mattia, C.A., Padiano, L.: Crystal structure of a new α-cyclodextrin hydrate form. Molecular geometry and packing features: disordered solvent contribution. Carbohydr. Res. **310**(1–2), 1–8 (1998)
7. Linder, K., Saenger, W.: Topography of cyclodextrin complexes. Part XVII. Crystal and molecular structure of cycloheptaamylose dodecahydrate. Carbohydr. Res. **99**, 103–115 (1982)
8. Saenger, W., Jacob, J., Gessler, K., Steiner, T., Hoffman, D., Sanbe, H., Koizumi, K., Smith, S.M., Takaha, T.: Structures of the common cyclodextrins and their larger analogues-beyond the doughnut. Chem. Rev. **98**, 1787–1802 (1998)
9. Harata, K.: The structure of the cyclodextrin complex. XX. Crystal structure of uncomplexed hydrated β-cyclodextrin. Bull. Chem. Soc. Jpn. **60**, 2763–2767 (1987)